

FAST X-RAY MICROTOMOGRAPHY FOR THE *IN SITU* ANALYSIS OF THE COMPRESSION OF A SATURATED FIBRE BUNDLE

P. Latil¹, L. Orgéas^{1,*}, C. Geindreau¹, S. Rolland du Roscoat¹, and P.J.J Dumont²

¹ CNRS – Université de Grenoble, Laboratoire Sos-Solides-Structures-Risques (3SR), BP 53, 38041 Grenoble Cedex 9, France : laurent.orgéas@grenoble-inp.fr

² CNRS – Grenoble INP, Laboratoire de Génie des Procédés Papetiers (LGP2), BP 65, 38402 Saint-Martin-d'Hères, France

ABSTRACT: X-Ray microtomography and image analysis tools are used to investigate the microstructure and the micromechanical behaviour of a saturated fibre bundle during a simple compression test. In order to achieve *in situ* observations of the microstructure evolution, the fast X-ray microtomography technique was performed at the ESRF. A methodology is then proposed to quantify from 3D images relevant microstructural descriptors which characterise the evolution of the fibrous medium during its deformation.

KEYWORDS: Micromechanics of fibre bundle - Fast X-Ray microtomography - *In situ* compression - Microstructure characterisation

INTRODUCTION

In recent years, the use of fibre-reinforced polymer composites in structural or functional applications has been increasing in industries such as automotive or aerospace. Most of the fibrous reinforcements of these materials are made up of continuous or discontinuous fibre bundles, so that they exhibit multiple scales: a macroscopic scale (the part scale), a mesoscopic scale (the fibre bundles scale) and a microscopic scale (the fibre scale). During the processing of composite materials, fibre bundles are usually subjected to very high deformations such as the shearing of dry woven textiles during their stamping in RTM process (Resin Transfer Moulding) [3], the bending and compression of wet short fibre bundle during the compression of GMT's or SMC's [4,5]. These mesoscale deformations induce very important and complex relative movements of fibres at the microscopic level. Such deformation mechanisms drastically affect the rheological behaviour of the composites during their processing by modifying the permeability and the anisotropy of the fibrous networks [2-5,7]. They also affect the final physical and mechanical properties of produced parts. Unfortunately, micro-deformation mechanisms are often complex and still not very well understood. For example, if deformations mechanisms at the bundle scale have already been studied experimentally for various fibrous reinforcements and various processing routes [2,4], much less is known on micro-deformation mechanisms within a fibre bundle during a given mechanical loading. This curbs the development of relevant constitutive bundle mesoscopic models [2]. Within this context, this study provides original experimental data concerning the evolution of the fibrous microstructure during the deformation of a saturated fibre bundle.

MATERIALS AND EXPERIMENTAL METHOD

A model fibre bundle was man-made. It consists of $N = 69$ rather aligned fibres (diameter $150\mu\text{m}$, length 12mm) which were extracted from a fluorocarbon continuous fishing wire. The bundle was saturated with olive oil, which behaves as a Newtonian fluid at room temperature (shear viscosity = 70mPa s) and which is solid at temperatures below 5°C . This characteristic allows the fixing of the fibrous microstructure of the bundle and facilitates its handling before mechanical testing performed at room temperature, *i.e.* when the oil is a fluid. Simple compression test was achieved with a specific compression micro-rheometer with a maximum axial load of 500N (see fig. 1 (a)) at a low strain rate, *i.e.* $\approx 5 \cdot 10^{-3} \text{ s}^{-1}$. The compression force F_2 and the current height of the sample l_2 were recorded during the test (see fig. 1(b)).

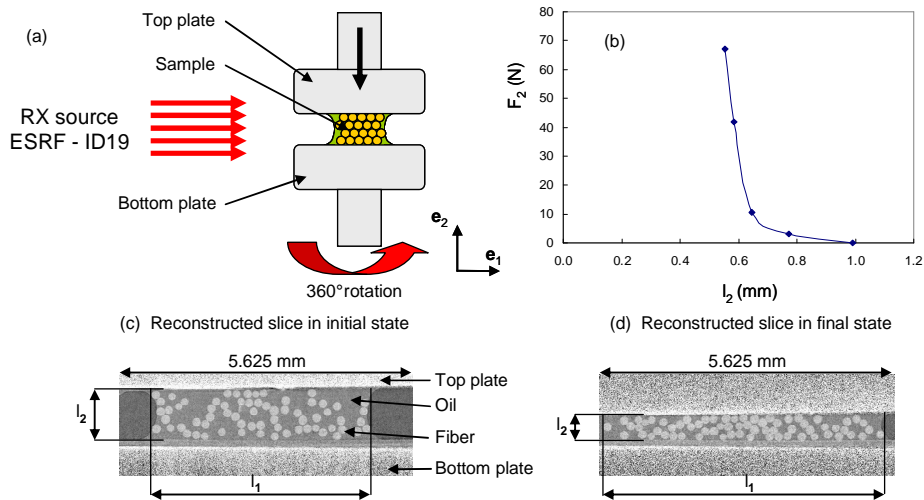


Fig. 1 – (a) Compression of the model fibre bundle, (b) Evolution of the compression force F_2 as a function of the sample height during the test. Reconstructed slice of the specimen in a plane parallel to $(\mathbf{e}_1, \mathbf{e}_2)$ in the initial (c) and final (d) states.

In order to characterise the 3D evolution of the fibre bundle microstructure during the compression test, the micro-rheometer was placed on a microtomograph at the ESRF (European Synchrotron Radiation Facility, ID19 beamline) in Grenoble. 3D images of the fibre bundle microstructure with a voxel size of $7.5 \mu\text{m}$ were performed by X-ray microtomography at five different levels of deformation. In order to limit possible microstructure evolution during the scan, the Fast Tomography technique was employed, allowing an acquisition time below 1 min [6]. The obtained 3D images allow to estimate and follow the volume occupied by fibres $V_f = l_1 \times l_2 \times l_3$ during the test (see fig. 1(c-d)).

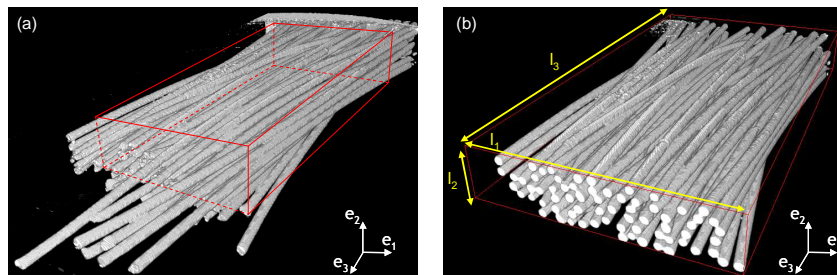


Fig. 2 – (a) Total scanned volume, (b) bundle volume under consideration.

The volume height l_2 is given by the distance between the two compression plates (fig. 1(c-d)). The width l_1 was chosen in order to contain all the fibres (see fig. 1(c-d) and fig. 2(b)). A similar hypothesis was done to estimate the length l_3 : due to the fibre length heterogeneity (induced by the elaboration protocol), we have arbitrarily truncated (about 1mm) the ends of some of the longest fibres which are not involved in the mechanical response of the bundle, as shown in figure 2(b).

For each level of deformation, the volume $V_f = l_1 \times l_2 \times l_3$ was determined, and thus the bundle stress (i) and the fibrous microstructure descriptors (ii) and (iii) were estimated:

- (i) The Cauchy stress component σ_{22f} of the fibrous medium was estimated assuming that the test was drained (very slow strain rate, negligible fluid pressure): $\sigma_{22f} \approx \sigma_{22} \approx F_2/(l_1 l_3)$.
- (ii) The volume fraction of fibres Φ was classically estimated after suitable filtering and thresholding operations which were performed with the 3D images of the volume V_f .
- (iii) In order to analyse more closely the fibrous architecture within the bundle (fibres and fibre-fibre contacts, see below). A method was developed for the identification and the individualisation of fibres. Hence, for each level of deformation, the volume V_f was divided into 10 slices along the \mathbf{e}_3 direction. On each slice, the centre of the cross section of each fibre was identified. Then for a given fibre, the positions of its ten centres were adjusted by a polynomial function (of a sufficient degree to minimize the errors) which characterises the fibre centreline. Thus, for each fibre, the local orientation (calculated from the tangent vector of the considered fibre), its tortuosity (here represented by the ratio of fibre length on the length of the chord joining the ends of the fibre) were evaluated. Fibre-fibre contacts were finally identified measuring the distance between the centrelines of neighbouring fibres.

RESULTS

- Fig. 1 (b) presents the evolution of compression force F_2 as a function of the sample height l_2 . From a qualitative point of view, this figure shows that the bundle was subjected to a pronounced consolidation which was accompanied with both liquid phase migration and an increase of the compression force.

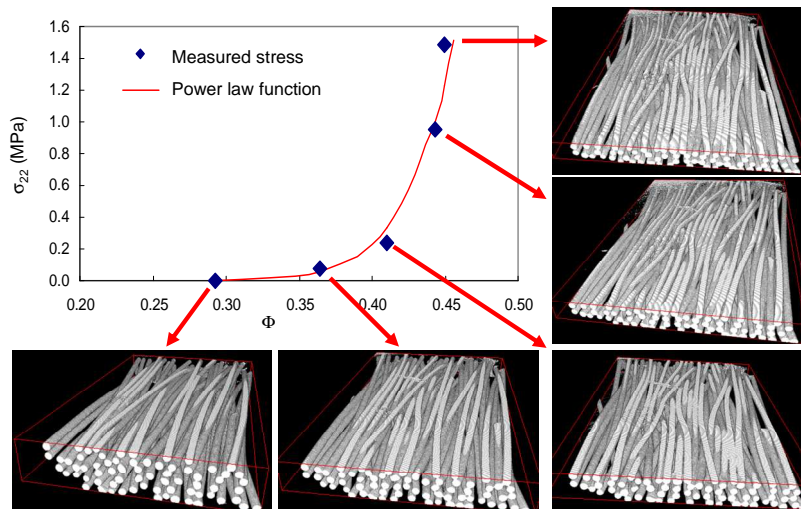


Fig. 3 – Evolution of the stress σ_{22f} as a function of volume fraction of fibres Φ , together with de various scanned volumes V_f observed at various deformation stages.

- The volume V_f corresponding to the five levels of compression are reported in Fig. 3 together with the evolution of the stress σ_{22f} as a function of the volume fraction of fibres Φ . This graph shows that the consolidation of the medium can be approximated by a phenomenological law often use in fibrous medium [8]: $\sigma_{22} = \alpha(\Phi^n - \Phi_0^n)$, where the values of α and n are respectively equal to $1.1 \cdot 10^5$ MPa and 14.25. These values are consistent with those of the literature [8].
- Whatever the compression deformation, the average tortuosity of each fibre is very close to 1 (about $2 \cdot 10^{-3}$). This allows considering that each fibre i is almost straight. A fibre orientation unit vector \mathbf{p}_i can thus be defined as the average of local tangent vectors of the fibre i .

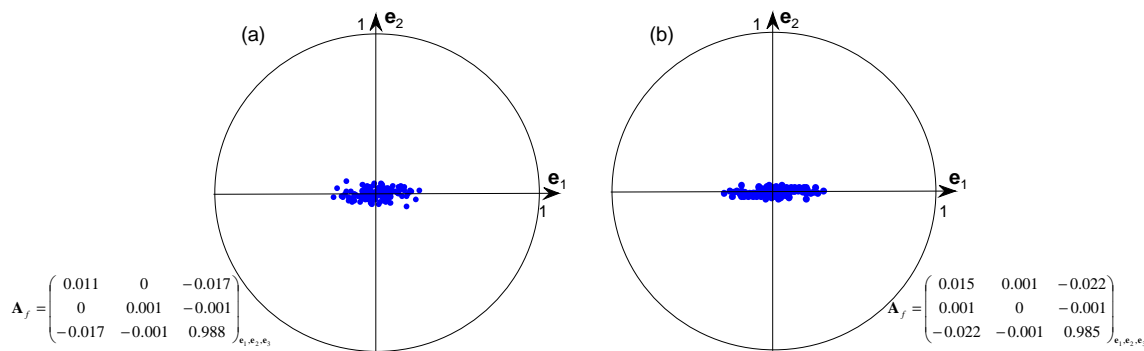


Fig. 4 – Pole figures (along \mathbf{e}_3) and associated fibre orientation tensors \mathbf{A}_f in the initial (a) and final (b) states.

- The fibre orientation vectors \mathbf{p}_i have been plotted in the pole figures shown in figure 4 for the initial and final states respectively. For each state, the corresponding value of the second order fibre orientation tensors $\mathbf{A}_f = 1/N \sum_{i=1}^N \mathbf{p}_i \otimes \mathbf{p}_i$ [1] was also computed from fibre orientation vectors \mathbf{p}_i . This figure shows that fibres in the initial state are mostly aligned along \mathbf{e}_3 , and that the disorientation is more pronounced in the plane $(\mathbf{e}_1, \mathbf{e}_3)$ than in $(\mathbf{e}_2, \mathbf{e}_3)$. These tendencies are accentuated by the compression.
- The observed increase of the volume fraction of fibres is accompanied with non-linear increase of the fibre-fibre contact number N_c (see fig. 5 (b)). Pole figures (a) and (c) and second order contact orientation tensors \mathbf{A}_c (Fig. 5) show that contacts are mostly oriented along \mathbf{e}_2 direction and that the compression increases this tendency.

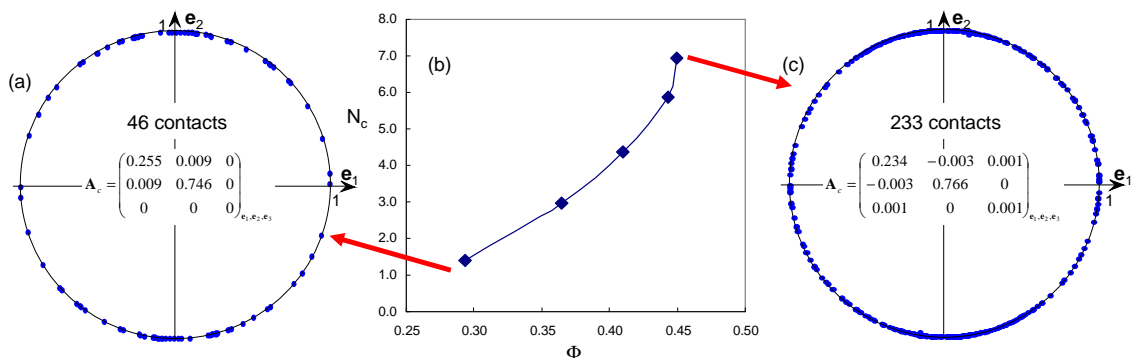


Fig. 5 – Evolution of the number fibre-fibre contacts N_c as a function of volume fraction of fibres Φ (b). Pole figures (along \mathbf{e}_3) and associated contact orientation tensors \mathbf{A}_c in the initial (a) and final (b) states.

CONCLUSIONS

The method developed in this work allowed a relatively fine description of micromechanisms involved during compression of a model fibre bundle. Some local descriptors related to fibres and their contacts have been estimated. Others may still be evaluated, such as bending of fibres (work in progress). Monitoring these descriptors during the bundle deformation will allow measuring the kinematic fields associated with the motion and the deformation of fibres and their contacts (work in progress). Taken together, these results should provide relevant data for theoretical or numerical models (discrete elements) describing the micromechanics of fibre bundles in the processing of polymer matrix composites.

ACKNOWLEDGMENTS

This work was performed within the framework of the ANR Jeunes Chercheurs “3D discrete Analysis of micromechanisms of deformation in highly concentrated fibre suspensions” (ANAFIB, ANR-09-JCJC-0030-01) and the ESRF LTP “Heterogeneous Fibrous Materials”. The authors also thank the cluster MACODEV for its financial support.

REFERENCES

- 1 S. G. Advani and C. L. Tucker, "The use of tensors to describe and predict fiber orientation in short fiber composites", *J. Rheol.*, 31, (1987), pp. 751-784
- 2 P. Badel, E. Vidal-Salle, E. Maire, P. Boisse, "Simulation and tomography analysis of textile composite reinforcement deformation at the mesoscopic scale.", *Compos. Sci. Technol.*, (2008), doi :10.1016/j.compositetech.2008.04.038.
- 3 P. Boisse “Meso-macro approach for composite forming simulation” *J. Mater. Sci.* 41 (2006) 6591-98.
- 4 P. Dumont, J.-P. Vassal, L. Orgéas, V. Michaud, D. Favier, J.A.E. Månson, "Processing, characterisation and rheology of transparent concentrated fibre bundle suspensions", *Rheol. Acta*, **46**, (2007), pp. 639-51.
- 5 T.H. Le, P.J.J. Dumont, L. Orgéas, D. Favier, L. Salvo, E. Boller, "X-ray phase contrast microtomography for the analysis of the fibrous microstructure of SMC composites", *Compos. Part A*, **39**, (2008), pp. 91-103.
- 6 N. Limodin, L. Salvo, M. Suéry, M. DiMichiel, "In situ investigation by X-Ray tomography of the overall and local microstructural changes occurring during partial remelting of an Al-15.8 wt.%Cu alloy.", *Acta Mater.*, **55**, (2007), pp. 3177-3191
- 7 F. Loix, L. Orgéas, C. Geindreau, P. Badel, P. Boisse, J.-F. Bloch “Flow of non-Newtonian liquid polymers through deformed composite reinforcements” *Compos. Sci. Technol.*, (2009), doi:10.1016/j.compscitech.2008.12.007
- 8 S. Toll, "Packing mechanics of fiber reinforcements", *Polym. Eng. Sci.*, **38**, 8, (1998), pp. 1337-1350.